多图谱与联合标签融合策略相结合的主动脉 CT 图像分割

摘　要：

Joint label fusion

D　　CT

15　　CT

D

关键词：　　3D　　CT

中图分类号：　TP391.41　　文献标志码：A

Multi-atlas Based Segmentation of Aortic CT Scans with Joint Label Fusion

Xu Yunlong[1]　Zheng Yuanjie[2]　Deng Xiang[1]　Li Ning[3]　Tang Yuchun[4]　, Yin Yilong[1]

(1. School of Computer Science and Technology, Shandong University, Jinan, 250101, China; 2. School of Information Science and Engineering, Shandong Normal University, Jinan, 250014, China; 3. Shandong Provincial Hospital, Jinan, 250021, China; 4. School of Medicine, Shandong University, Jinan, 250012, China)

Abstract: Automatic aortic image segmentation plays an important role in early aortic disease diagnosis, risk evaluation and treatment planning. In this paper, we use a multi-atlas based medical image segmentation method and first combine it with a joint label fusion strategy to segment 3D aortic CT images automatically. Joint label fusion strategy takes the correlation of atlases into consideration and the effect of redundant information of atlases can be restrained. To handle the problem of insufficient atlases, we propose an atlas archive update method which can enhance the segmentation accuracy with relatively low computational complexity. We evaluate our method by using a data set with 15 aortic subject and comparing with three widely used label fusion techniques (majority voting, local-weighted label fusion and STAPLE). Experimental results show superior performances of our method to state-of-the-art.

基金项目：

收稿日期：　　修订日期：

Key words: multi-atlas segmentation; joint label fusion strategy; aortic CT image; atlas archive update

引　　言

MRI　　CT　　US

3D

Snakes

Contour

CT

3D

target image

majority

voting

weighted voting

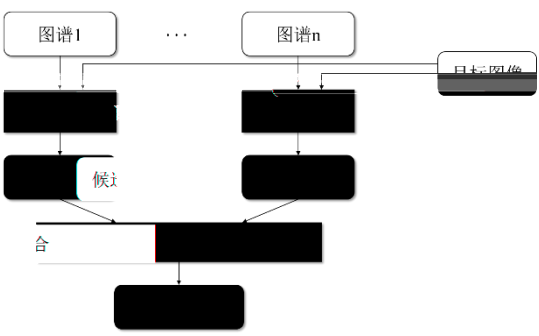

Fig. 1 Flowchart of atlas based medical image segmentation

3D　　CT

1　基于多图谱与联合标签融合的主动脉 CT 图像分割技术

1.1 图谱选择

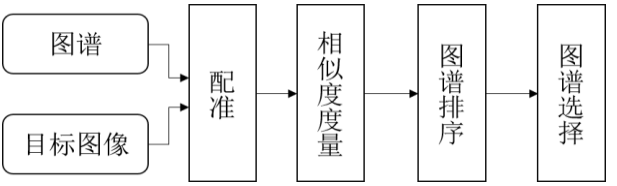

Fig. 2 Flowchart of atlas selection

mutual information

CT　　CT

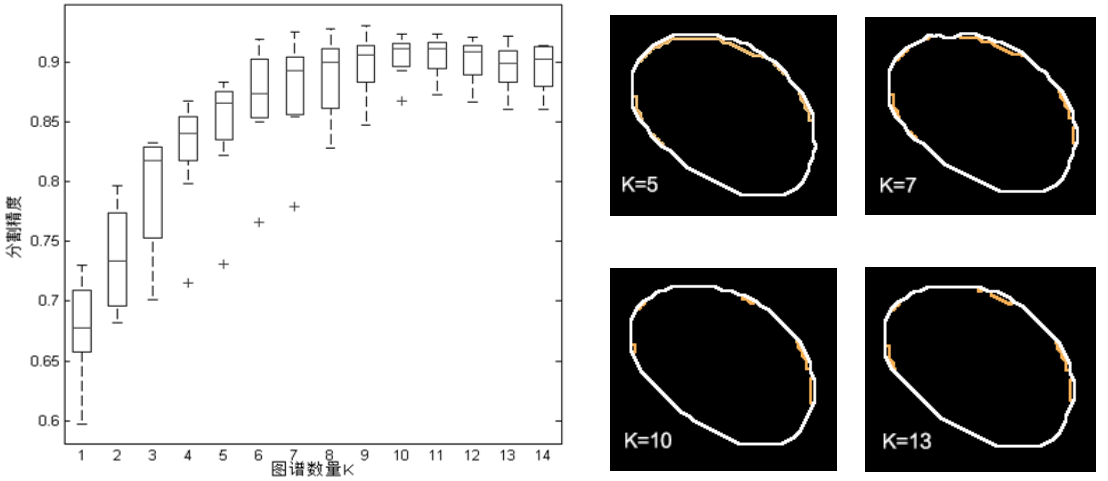

K

ground truth

Fig.3 Performance of different number of atlases. Left: The box-whisker plot of the dice coefficient with different number of atlases. Right: Segmentation results with 5, 7, 10 and 13 atlases, respectively.

K

K

5 10

K=10

1.2 图谱更新

60

I_T A_i $Sim(I_T, A_i)$ $i = 1,2, \dots, n$ n $Sim(I_T, A_i)$ ε

template

ANTs

1.3 图像配准

σ voxel Convergence convergence

ANTs symmetric image normalization method (Syn) Syn

σ voxel Syn

Convergence convergence

1.4 联合标签融合

Joint label fusion JLF

STAPLE

LWGaussian LWInverse

I_T $S_T(x)$ I_T $A = \{A_i | \, i = 1,2, \dots, n\}$

n $A_i = (I_i, S_i)$ I_i S_i i

voxel

$$\delta^i(x) = S_i(x) - S_T(x)$$

$\delta^i(x)$ i x

x

$$S(x) = \sum_{i=1}^{n} w_i(x) \, S_i(x)$$

$\sum_{i=1}^{n} w_i(x) = 1$ $S(x)$ $S_T(x)$

$S(x)$ $S_T(x)$

$$\begin{aligned} & E_{\delta^1(x),\dots,\delta^n(x)}[(S_T(x) - S(x))^2 | I_T, I_1, \dots, I_n] \\ &= E_{\delta^1(x),\dots,\delta^n(x)}\left[(\sum_{i=1}^{n} w_i(x)\delta^i(x))^2 | I_T, I_1, \dots, I_n\right] \\ &= \sum_{i=1}^{n}\sum_{i=1}^{n} w_i(x) \, w_j(x) \, E_{\delta^i(x),\delta^j(x)}[\delta^i(x), \delta^j(x) | I_T, I_1, \dots, \, I_n] \\ &= \mathbf{w}_x^t M_x \mathbf{w}_x \end{aligned}$$

$\mathbf{w}_x$ M_x $n * n$ $M_x(i,j)$ i j

x M_x

$$M_x(i,j) = E_{\delta^i(x),\delta^j(x)}\left[\left[\delta^i(x), \delta^j(x) \mid I_T, I_1, \dots, I_n\right] = p(\delta^i(x)\delta^j(x) = 1 \mid I_T, I_1, \dots, I_n\right)$$

M_x

$$M_x(i,j) \sim [\, \textstyle\sum_{y \in \mathcal{N}(x)} |I_T(y) - I_i(y)| \, \big|I_T(y) - I_j(y)\big| \,]^{\beta}$$

$\mathcal{N}(x)$ x β

$\sum_{i=1}^{n} w_i(x) = 1$ $\mathbf{w}_x^t M_x \mathbf{w}_x$

$$w_x^* = argmin \, \mathbf{w}_x^t M_x \mathbf{w}_x \quad \text{s.t.} \quad \sum_{i=1}^{n} w_i(x) = 1 \qquad 6$$

$$\mathbf{w}_x = \frac{M_x^{-1} 1_n}{1_n^t M_x^{-1} 1_n}$$

$1_n = [1; 1; \dots; 1]$ n w_x^*

$$w_x^* = argmin \, \mathbf{w}_x^t (M_x + \alpha I) \mathbf{w}_x \quad \text{s.t.} \quad \sum_{i=1}^{n} w_i(x) = 1$$

α

2 实验结果与分析

2.1 实验数据与预处理

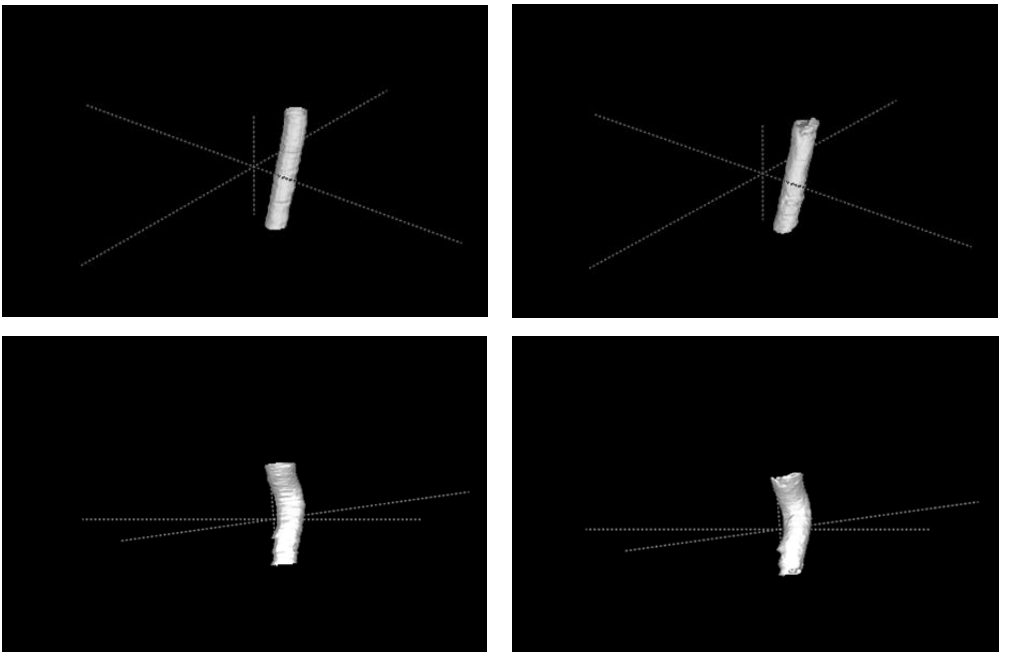

Fig. 4 3D segmentation results with the proposed method. Left column: Ground truth. Right column: Segmentation using the proposed method.

15 3D CT CT Siemens SOMATOM Definition Flash scanner KVp ×
5mm 16bits/pixel × ×
ITK-SNAP
ImageJ

3D CT
origin voxel spacing

2.2 实验实现及评估

leave-one-out
ANTs E5
64GB

3D CT ground truth

majority voting MV STAPLE Simultaneous truth and performance level estimation local weighted fusion LW joint label fusion JLF dice similarity coefficient DSC DSC ground truth

$$DSC(S,G) = \frac{2\cdot \|S\cap G\|}{\|S\|+\|G\|}$$

ground truth

3D CT ±

STAPLE MV LW

Tab.1 Average performance of different label fusion strategies in aortic CT scans segmentation

	(JLF)	MV	STAPLE	LW
Dice coefficient	**0.904±0.018**	0.859±0.046	0.878±0.037	0.895±0.023

Tab.2 Segmentation accuracy with and without the atlas update process

Dice coefficient	Atlas 6	0.817±0.047	**0.863±0.033**
	Atlas 8	0.834±0.038	**0.872±0.026**

Atlas Atlas

Atlas Atlas

3 结束语

Joint label fusion

3D CT

3D CT

3D

参考文献：

[1] Kochanek K D, Xu J, Murphy S L, et al. Deaths: final data for 2009[J]. National vital statistics reports: from the Centers for Disease Control and Prevention, National Center for Health Statistics, National Vital Statistics System, 2011, 60(3): 1-116.

[2] Ayed I B, Wang M, Miles B, et al. TRIC: Trust Region for Invariant Compactness and Its Application to Abdominal Aorta Segmentation [M]//Medical Image Computing and Computer-Assisted Intervention–MICCAI 2014. Springer International Publishing, 2014: 381-388.

[3] Rueckert D, Burger P, Forbat S M, et al. Automatic tracking of the aorta in cardiovascular MR images using deformable models[J]. Medical Imaging, IEEE Transactions on, 1997, 16(5): 581-590.

[4] Zhuge F, Rubin G D, Sun S, et al. An abdominal aortic aneurysm segmentation method: level set with region and statistical information [J]. Medical physics, 2006, 33(5): 1440-1453.

[5] , , , . [J]. , 2015, 30(2): 350-358.
Lu Xiaoqi, Shi Jing, Ren Xiaoying, et al. Hybrid segmentation for 3D liver magnetic resonance imaging based on level set method[J]. Journal of Data Acquisition and Processing, 2015, 30(2): 350-358.

[6] , , . [J]. , 2014, 29(5): 704-712.
Tang Liming, Huang Darong, Li Keren. New model based on variational level set for image segmentation[J]. Journal of Data Acquisition and Processing, 2014, 29(5), 704-712.

[7] Mikić I, Krucinski S, Thomas J D. Segmentation and tracking in echocardiographic sequences: active contours guided by optical flow estimates[J]. Medical Imaging, IEEE Transactions on, 1998, 17(2): 274-284.

[8] Išgum I, Staring M, Rutten A, et al. Multi-atlas-based segmentation with local decision fusion—application to cardiac and aortic segmentation in CT scans[J]. Medical Imaging, IEEE Transactions on, 2009, 28(7): 1000-1010.

[9] , , , . MRI [J]. , 2015,30(5): 956-964.
He Xiaohai, Liang Zifei, Tang Xiaoying, et al. Development and application for atlas-based brain MRI image segmentation technology[J]. Journal of Data Acquisition and Processing, 2015, 30(5): 956-964

[10] Collins D L, Pruessner J C. Towards accurate, automatic segmentation of the hippocampus and amygdala from MRI by augmenting ANIMAL with a template library and label fusion[J]. Neuroimage, 2010, 52(4): 1355-1366.

[11] Artaechevarria X, Munoz-Barrutia A, Ortiz-de-Solórzano C. Combination strategies in multi-atlas image segmentation: Application to brain MR data[J]. Medical Imaging, IEEE Transactions on, 2009, 28(8): 1266-1277.

[12] Heckemann R A, Hajnal J V, Aljabar P, et al. Automatic anatomical brain MRI segmentation combining label propagation and decision fusion[J]. NeuroImage, 2006, 33(1): 115-126.

[13] Wang H, Suh J W, Das S R, et al. Multi-atlas segmentation with joint label fusion[J]. Pattern Analysis and Machine Intelligence, IEEE Transactions on, 2013, 35(3): 611-623.

[14] Sanroma G, Wu G, Gao Y, et al. Learning to rank atlases for multiple-atlas segmentation[J]. Medical Imaging,IEEE Transactions on, 2014, 33(10): 1939-1953.

[15] Elnakib A, Gimel'farb G, Suri J S, et al. Medical image segmentation: a brief survey[M]. Multi ModalityState-of-the-Art Medical Image Segmentation and Registration Methodologies. Springer New York, 2011: 1-39.

[16] Avants B B, Tustison N, Song G. Advanced normalization tools (ANTS)[J]. Insight J, 2009, 2: 1-35.

[17] Avants B B, Epstein C L, Grossman M, et al. Symmetric diffeomorphic image registration with cross-correlation:evaluating automated labeling of elderly and neurodegenerative brain[J]. Medical image analysis, 2008, 12(1): 26-41.

[18] Warfield S K, Zou K H, Wells W M. Simultaneous truth and performance level estimation (STAPLE): an algorithm for the validation of image segmentation[J]. Medical Imaging, IEEE Transactions on, 2004, 23(7): 903-921.